Multiexciton Absorption Cross Sections of CdSe@CdS Nanorods Studied Using Pump-rePump-Probe Spectroscopy

Krishan Kumar[1,2,#], Jens Uhlig[3], Raktim Baruah[1,2,4†], Shivani Yadav[1,4], Maria Wächtler[2]*†*

[1]Department Functional Interfaces, Leibniz Institute of Photonic Technology Jena, Albert-Einstein-Straße 9, 07745 Jena, Germany

[2]Chemistry Department and State Research Center OPTIMAS, RPTU Kaiserslautern-Landau, Erwin-Schrödinger-Str. 52, 67663 Kaiserslautern

[3]Division of Chemical Physics, Department of Chemistry, Lund University, Box 124, SE-22100 Lund, Sweden; NanoLund, Lund University, 22100 Lund, Sweden; LINXS Institute of Advanced Neutron and X-Ray Science, Lund University, 22370 Lund, Sweden

[4]Institute of Physical Chemistry, Friedrich Schiller University Jena, Lessingstraße 8, 07743 Jena, Germany

Current Address

[#] Institut für Physik, Carl von Ossietzky Universität Oldenburg, 26129 Oldenburg, Germany

[†] Institute of Physical Chemistry and Kiel Nano, Surface and Interface Science (KiNSIS), Christian-Albrechts-Universität zu Kiel, Max-Eyth-Straße 1, 24118 Kiel

Corresponding Authors

*Email: krishan.kumar@uni-oldenburg.de, waechtler@phc.uni-kiel.de

Absorption spectrum of nanorods

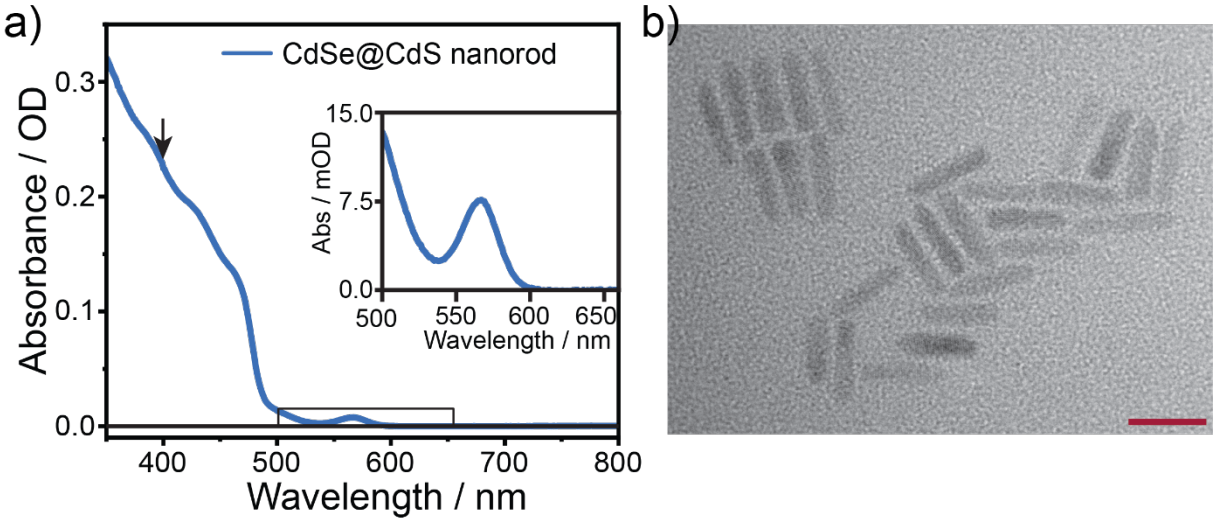

Figure S1. a) Typical absorption spectrum of CdSe@CdS nanorods dispersed in toluene. The arrow represents the excitation wavelength used in ppp-TA spectroscopic measurements. b) TEM images of CdSe@CdS nanorods used in the study. The scale bar shown in red is 20 nm.

The characteristic absorption spectrum of CdSe@CdS nanorods in toluene is presented in Figure S1, showing excitonic transitions localised in the CdSe seed around 565 nm (inset), as well as a $1\sum$ exciton transition around 467 nm and a $1\prod$ exciton transition around 429 nm which are related to the CdS nanorod region. Besides these pronounced features, the absorption spectra also show a small peak around 507 nm, which is assigned to a transition forming an excitonic state localised at the interface of the CdS rod and CdSe seed, also referred to as the bulb region in these seeded nanorods.[1,2]

Modelling of ppp-TA experimental data

The non-radiative Auger recombination of multiexcitons occurs via a sequential cascade mechanism, as established in the literature.[3,4] Briefly, the initially generated Nth order multiexciton (N being the number of excitons generated in one nanorod) decays to form (N–1)th order multiexciton, which decays to a (N–2)th order multiexciton and so on. The rate laws for such a scheme can be written as

$$\begin{aligned} \frac{d[N]}{dt} &= -\frac{[N]}{\tau_N} \\ \frac{d[N-1]}{dt} &= \frac{[N]}{\tau_N} - \frac{[N-1]}{\tau_{N-1}} \\ \frac{d[N-2]}{dt} &= \frac{[N-1]}{\tau_{N-1}} - \frac{[N-2]}{\tau_{N-2}} \\ &\cdots \\ \frac{d[1]}{dt} &= \frac{[2]}{\tau_2} - \frac{[1]}{\tau_1} \end{aligned} \tag{1}$$

with τ_N being the lifetime of the Nth order multiexcitonic state. The initial population of the multiexcitons in an ensemble of nanorods generated by the absorption of light follows a Poisson distribution:

$$P_N(0) = \frac{< N >^N e^{-<N>}}{N!} \tag{2}$$

where $< N >$ is the average number of excitons per nanorod, which depends on the excitation pump intensity and can be determined from the average energy density (J in Photons/cm^2) and an absorption cross-section scaled with the pump power density parameter (σ_1) in cm^2

$$< N >= \mathrm{J} \times \sigma_1 \tag{3}$$

Hence, with equations 2 and 3, the excitation intensity-dependent starting concentrations $c_N(t = 0, J)$ of contributing monoexcitonic and multiexcitonic states of different order can be described. Based on the absorption cross-section ($\sigma_1 = 4.14 \times 10^{-15}$ cm^2) determined previously in

intensity-dependent pump-probe experiments[5] and 1st pump intensity, the initial population distribution can be modelled as

$$\begin{aligned} [GS] &= \mathrm{P_{N=0}}(0) \\ [X] &= \mathrm{P_{N=1}}(0) \\ [BX] &= \mathrm{P_{N=2}}(0) \\ [TX] &= \mathrm{P_{N=3}}(0) \\ [QX] &= 1 - \mathrm{P_{N=3}}(0) - \mathrm{P_{N=2}}(0) - \mathrm{P_{N=1}}(0) - \mathrm{P_{N=0}}(0) \end{aligned} \tag{4}$$

where GS, X, BX, TX, and QX denote the initial concentration of ground state, monoexciton, biexciton, triexciton and tetraexciton respectively. The total number of species required to explain the pump-probe transient absorption data in the measured intensity range is 4, as determined previously.[5]

To incorporate the interaction of repump pulse, the initial concentration of various excitonic states (given by Poisson distribution dependent on σ) evolves as per the rate laws given in equation (1), and the time of repump of the population of various excitonic states is redistributed as per another absorption cross-section parameters (σ_{GS}, σ_X, σ_{BX} … for absorption cross-section parameter for ground state and multiexcitonic states upon interaction with repump pulse).

For repump interacting with mono- and biexciton species (which corresponds to 500 ps delay) it follows:

For ground state reexcitation:

$$P'_N(repump) = \frac{(\mathrm{J_{repump}} \times \sigma_{GS})^N e^{-(\mathrm{J_{repump}} \times \sigma_{GS})}}{N!} \tag{5}$$

$P'_N(repump)$ denotes the Poisson contribution to the distribution of N[th] order exciton for the interaction with repump pulse with the ground state species.

For monoexciton reexcitation:

$$P''_N(repump) = \frac{(\mathrm{J_{repump}} \times \sigma_{X})^N e^{-(\mathrm{J_{repump}} \times \sigma_{X})}}{N!} \tag{6}$$

where $P_N''(repump)$denotes the contribution according to the Poisson distribution of Nth order exciton for the interaction with repump pulse.

So overall the population change after repump interaction can be modelled as

$$[GS]_{repump} = [GS]_{\mathrm{t}} - \Big([GS]_{\mathrm{t}} \times \big(1 - P_0'(repump)\big)\Big)$$

$$\begin{aligned}[X]_{repump} = [\mathrm{X}]_{\mathrm{t}} &- \Big([\mathrm{X}]_{\mathrm{t}} \times \big(1 - P_0''(repump)\big)\Big) \\ &+ \Big([\mathrm{GS}]_{\mathrm{repump}} \times P_1'(repump)\Big)\end{aligned}$$

$$\begin{aligned}[BX]_{repump} = [\mathrm{BX}]_{\mathrm{t}} &+ [\mathrm{X}]_{\mathrm{t}} \times P_1''(repump) \\ &+ \Big([\mathrm{GS}]_{\mathrm{repump}} \times P_2'(repump)\Big)\end{aligned} \tag{7}$$

$$\begin{aligned}[TX]_{repump} = [\mathrm{TX}]_{\mathrm{t}} &+ \big([X]_t \times P_2''(repump)\big) \\ &+ \Big([\mathrm{GS}]_{\mathrm{repump}} \times P_3'(repump)\Big)\end{aligned}$$

$$\begin{aligned}[QX]_{repump} = [\mathrm{QX}]_{\mathrm{t}} &\left([X]_t \times \left(1 - \sum_{i=0}^{2} P_i''(repump)\right)\right) \\ &+ \left([\mathrm{GS}]_{\mathrm{repump}} \times \left(1 - \sum_{i=0}^{3} P_i'(repump)\right)\right)\end{aligned}$$

where *t* subscript denotes the concentration of that species right before the repump arrival time, and subscript *repump* denotes the concentration of that species after the repump interaction. Thus, equations 5–7 allow the redistribution of higher order exciton population after the repump interaction, which then evolves with the same rate law equation described in equation (1). To simplify the redistribution of concentration and since the intensity of repump pulse is sufficiently low, we only allowed a maximum absorption of two photons from the given state of interaction, i.e., formation of up to biexciton when repump pulse interacts with ground state species (see Figure

S3) and hence formation of triexciton when repump pulse interacts with monoexciton species and so on. Assuming the species spectra for the various contributing species $s_N(\lambda)$ are not changing with time or the repump excitation intensity and that the observed decay kinetic solely is influenced by the evolving population and repump interaction only results in population redistribution among the contributing states, the ppp-TA data can be simulated

$$\Delta A(\lambda, t, J) = \sum_{N=1}^{4} c_N(t, J) s_N(\lambda) \qquad (4)$$

Modelling the repump excitation intensity-dependent ppp-TA dataset for all repump intensities simultaneously, the lifetimes τ_N, the absorptions cross-section parameters for higher order excitons σ_X & σ_{GS}, and the component spectra $s_N(\lambda)$ of the species can be determined using the MCMC sampling method for target analysis.[6]

For shorter delay between pump and repump the approach is similar taking into account additionally reexcitation of bi- and tri-excitons in the ensemble respectively.

Experimental results – 500 ps re-excitation

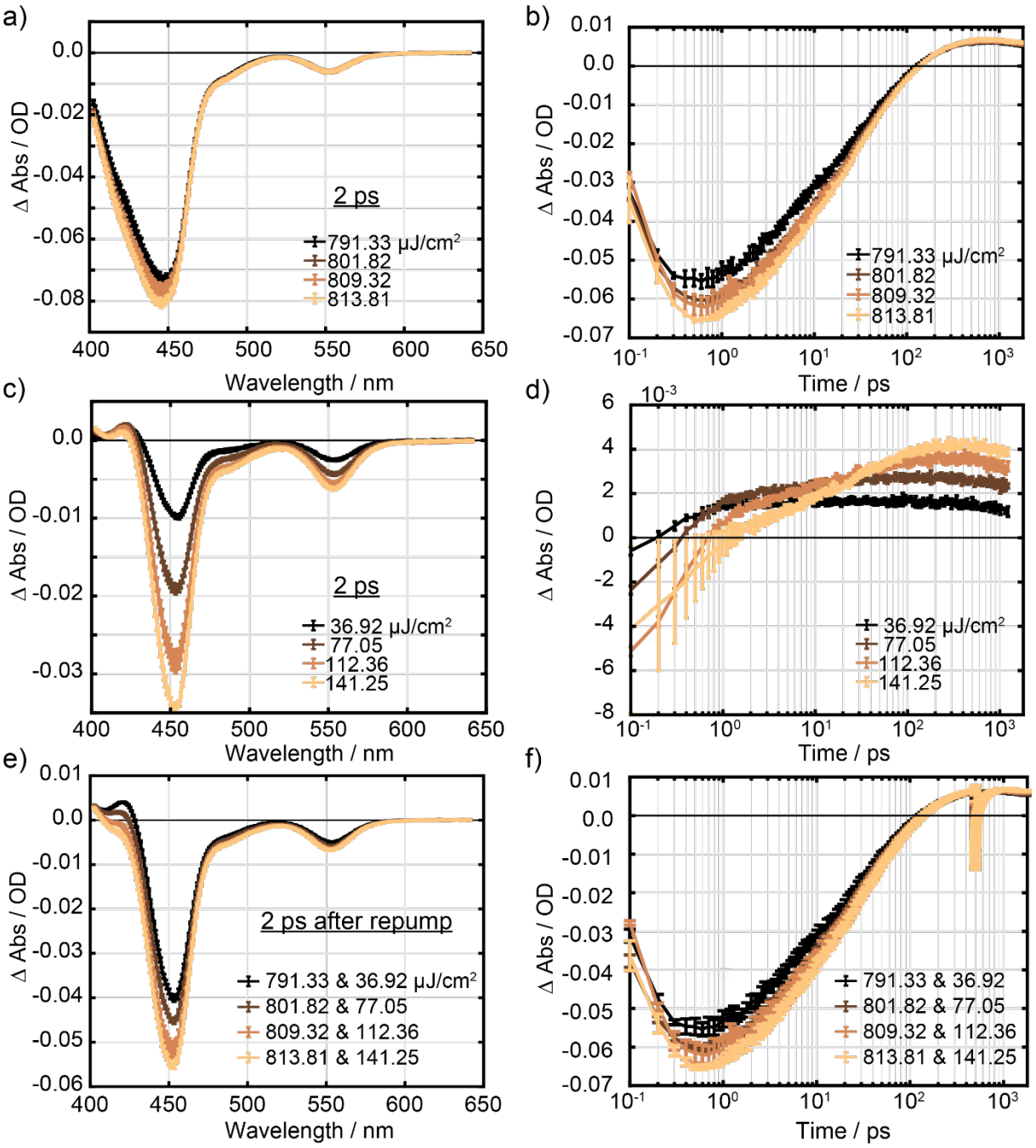

Figure S2. Reference experiments for 500 ps pump repump delay experiment of main text. pp-TA data of CdSe@CdS nanorods excited with pump (a & b), repump pulse (c & d) only and ppp-TA data for direct comparison (e & f). (a,b) pp-TA spectra of nanorods at 2 ps after the pump pulse

excitation and kinetics of 423 nm band with pump intensity shown in legend. (c,d) pp-TA spectra of nanorods at 2 ps after repump excitation and kinetics of photoinduced band at 423 nm with increasing repump intensity as shown in the legends. The time of arrival of the repump pulse is corrected by subtracting the original pump-repump delay having the excitation event at 0 ps. (e,f) ppp-TA spectra of nanorods at 2 ps after excitation with the repump pulse and the kinetics of 423 nm band. The panel e & f are same as shown in Figure 1 of main text except panel f shows data plotted on log scale.

Figure S2a shows the pp-TA data obtained using first pump pulse only. The spectral features shown here have been explained earlier,[5] briefly the TA spectra shows a bleach around 450 nm and 553 nm corresponding to the lowest energy transition localized in CdS and CdSe domains respectively. The 450 nm bleach feature extends further into high energy regions which shows the presence of excitons in higher energy band levels along with band-edge exciton. Hence, the kinetics of higher energy band (423 nm) sensitively reports on the presence of multiple excitons in these systems as shown in Figure S2b. In ~500 ps the TA signal reaches a saturating maximum signal representing the decay of all higher order exciton by Auger recombination to form monoexciton species. Hence 500 ps have been used as the pump-repump delay to mainly target monoexciton state. Similar TA features can be observed when excited with repump pulse only, Figure S2c&d. The significant differences can be seen in the higher energy region, i.e., below 450 nm. At lower repump intensity, a photoinduced absorption band is observed at 423 nm, which is due to the biexcitonic effect observed by interaction of probe pulse interaction with the monoexciton species generated by the repump pulse excitation. At the lowest repump intensity the 423 nm kinetics (Figure S2d) show maximum positive signal formation in < 1 ps after excitation and with increasing repump intensity the TA signal first shows a negative signal which then

recovers to form a positive signal over delay time. Hence the reference experiment, especially at lowest repump intensity, shows that interaction of repump pulse with ground state nanorod species would majorly generate monoexciton species only. Thereby, if the repump pulse only interacts with ground state species in the ppp-TA experiment (Figure S2e, f or Figure 1) would generate monoexciton and should result in net increase of 423 nm signal after ~1 ps of repump interaction. However, the experimental ppp-TA data clearly show a decrease in PA signal after 2 ps of repump interaction in ppp-TA experiment which clearly shows the interaction of repump pulse is not alone with ground state but also with monoexciton species as well.

ppp-TA data for CdS and CdSe bleach feature

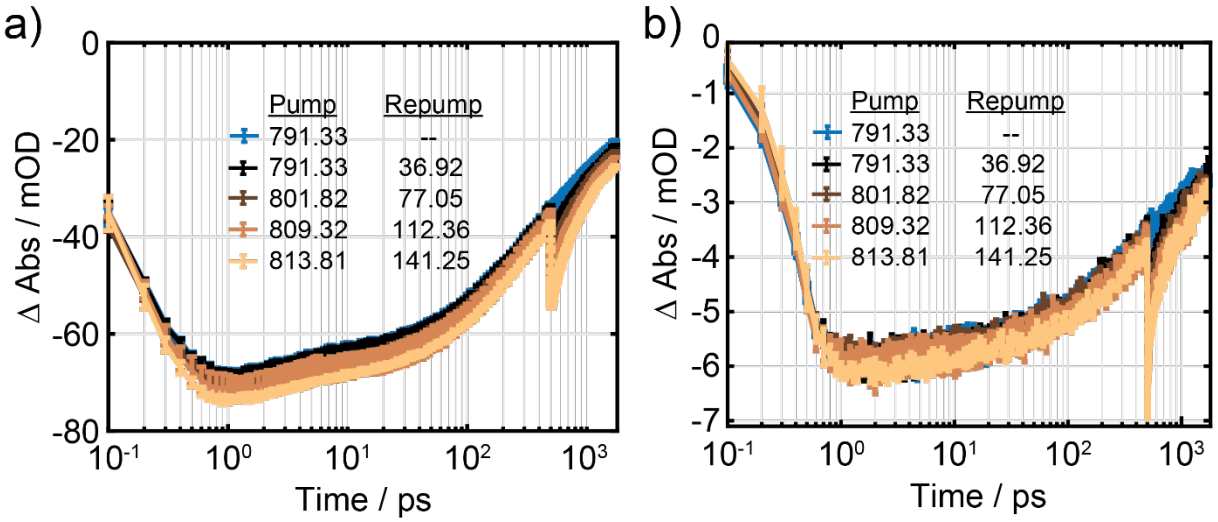

Figure S3. ppp-TA kinetics of CdS and CdSe band edge bleach features at 455 (a) and 553 nm (b), respectively with varying re-excitation intensity as shown in the legend for 500 ps re-excitation. Representative pp-TA kinetics of the same band have also been plotted for comparison in blue (pump intensity 791.33 μJ/cm^2).

Fitting results – 500 ps re-excitation

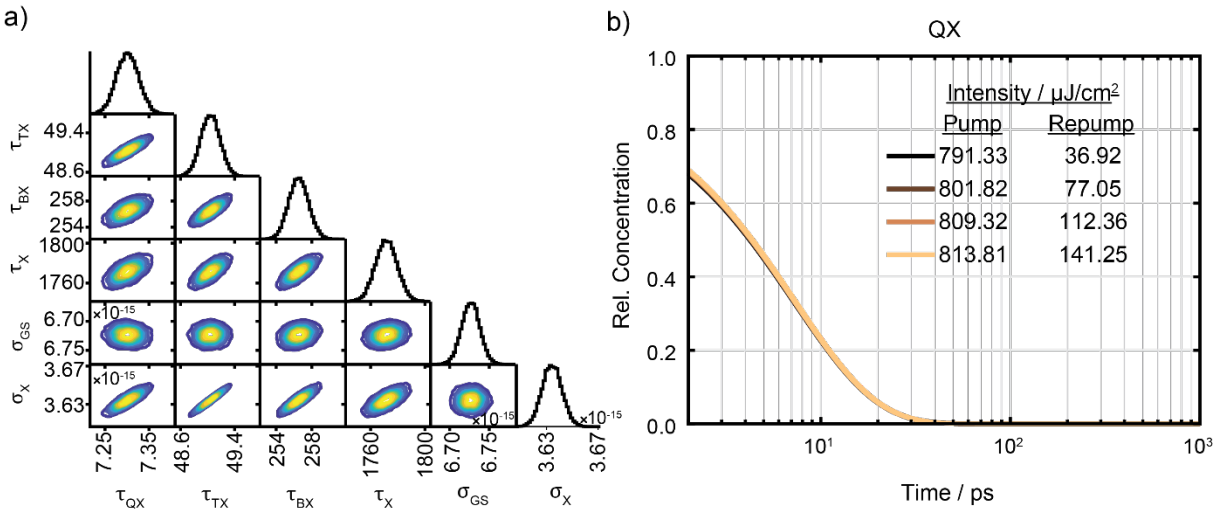

Figure S4. Markov Chain Monte Carlo (MCMC) sampling of monoexciton re-excitation (500 ps delay between pump-repump pulse) experimental data for TOPO-capped CdSe@CdS nanorods. (a) Corner plot of the posterior probability distribution of modelled parameters obtained from MCMC sampling of the target model for pump intensity > 790 µJ/cm^2 and re-pump intensity ranging from ~37 – 141 µJ/cm^2, (b) Concentration profile of modelled tetraexciton species, remaining concentration profiles are shown in the main text. Each curve in the concentration profile has been plotted from 100 random samples drawn from the MCMC sampling.

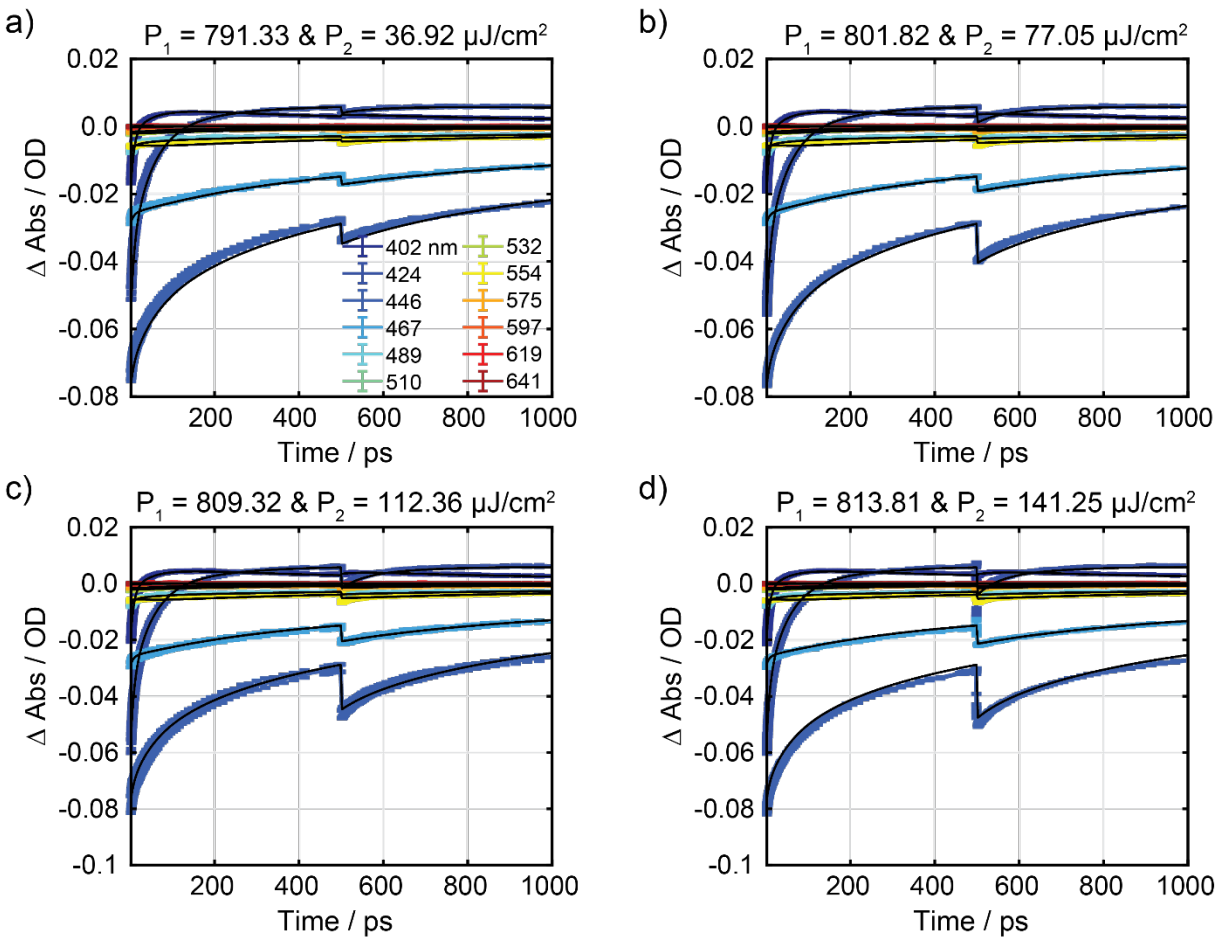

Figure S5. (a-d) Kinetics fits drawn from MCMC sampling of target model for monoexciton re-excitation (500 ps delay between pump-repump pulse). Each panel shows the experimental data with their standard deviation over at least 4 scans, and black lines represent the kinetic fit traces at that pump/repump intensity. The fit lines are plotted by drawing 100 random samples from the Markov Chain overlaid on top of each other with the same colour and linewidth to visually show the deviations among randomly drawn samples.

Experimental results – 70 ps re-excitation

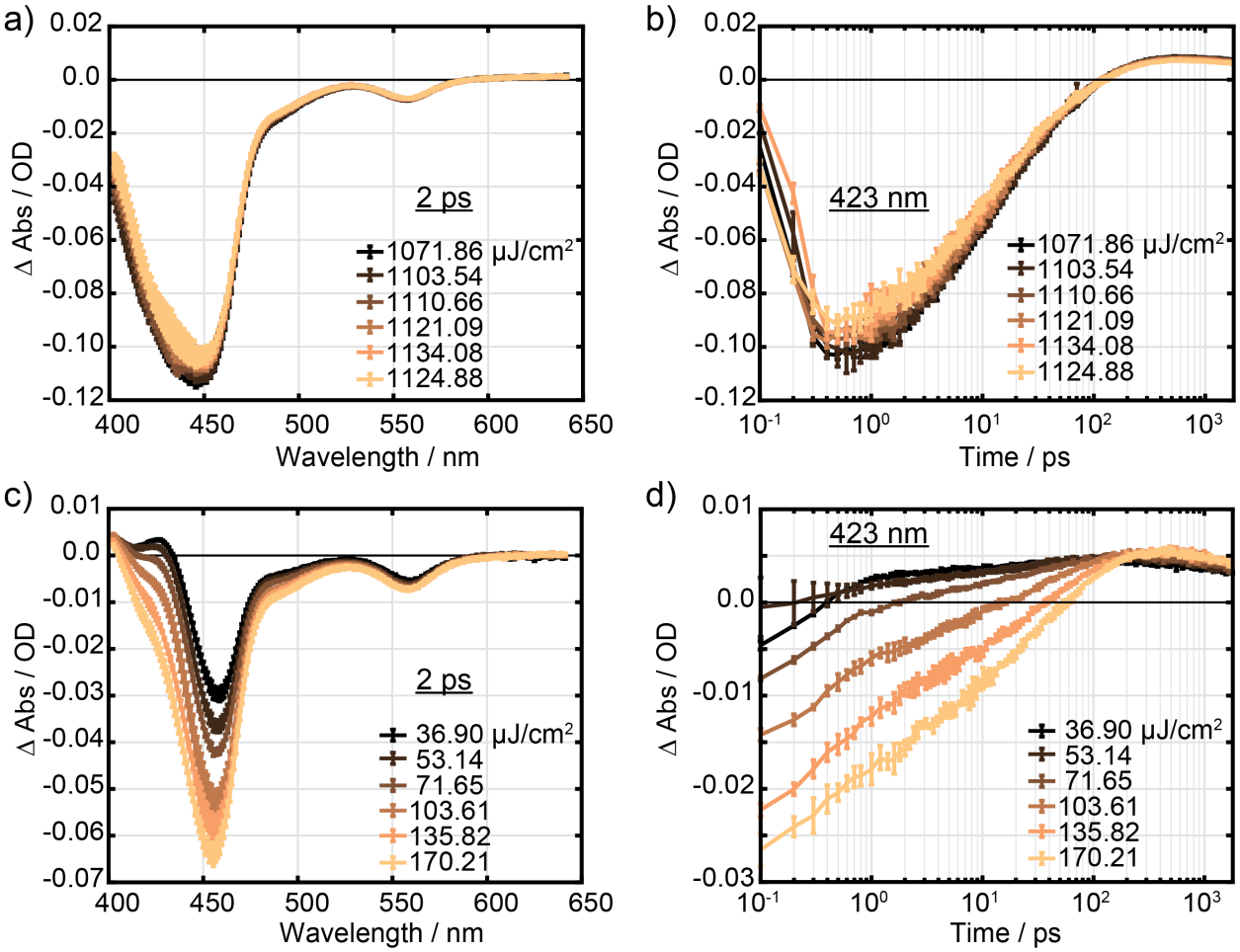

Figure S6. Reference experiments for 70 ps pump repump delay experiment of main text. pp-TA data of CdSe@CdS nanorods excited with pump (a & b) and repump pulse (c & d) only. (a,b) pp-TA spectrum of nanorods at 2 ps after the pump pulse excitation and kinetics of 423 nm band with pump intensity shown in legend. (c,d) pp-TA spectrum of nanorods at 2 ps after repump excitation and kinetics of photoinduced band at 423 nm with increasing repump intensity as shown in the legends. The time of arrival of the repump pulse is corrected by subtracting the original pump-repump delay having the excitation event at 0 ps.

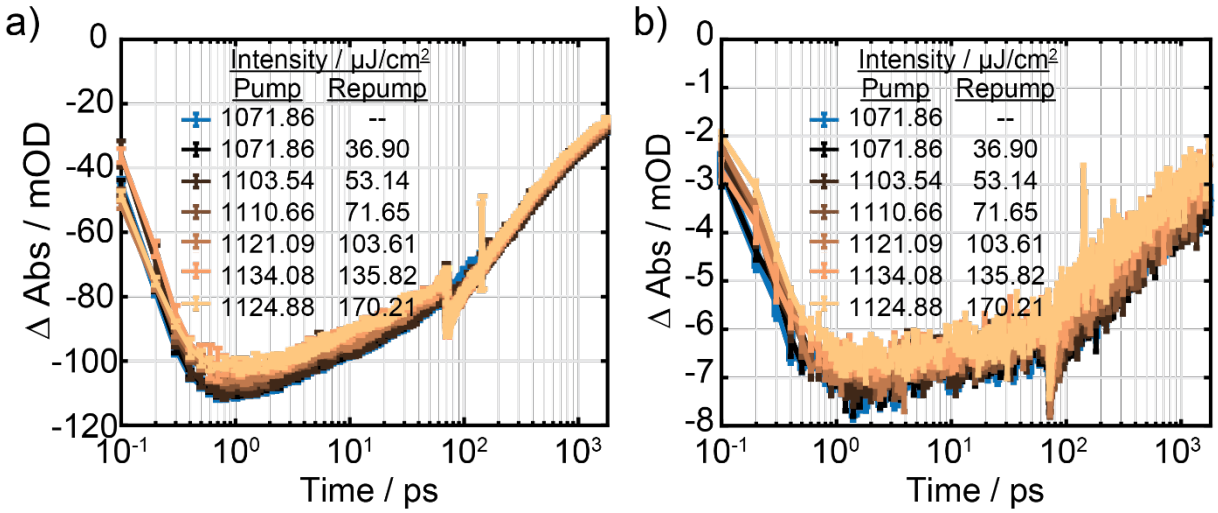

Figure S7. ppp-TA kinetics of CdS and CdSe band edge bleach features at 455 nm (a) and 553 nm (b), with varying re-excitation intensity as shown in the legend, along with a representative pp-TA kinetics of the same band shown in blue (pump intensity 1071.86 μJ/cm^2).

Fitting results – 70 ps re-excitation

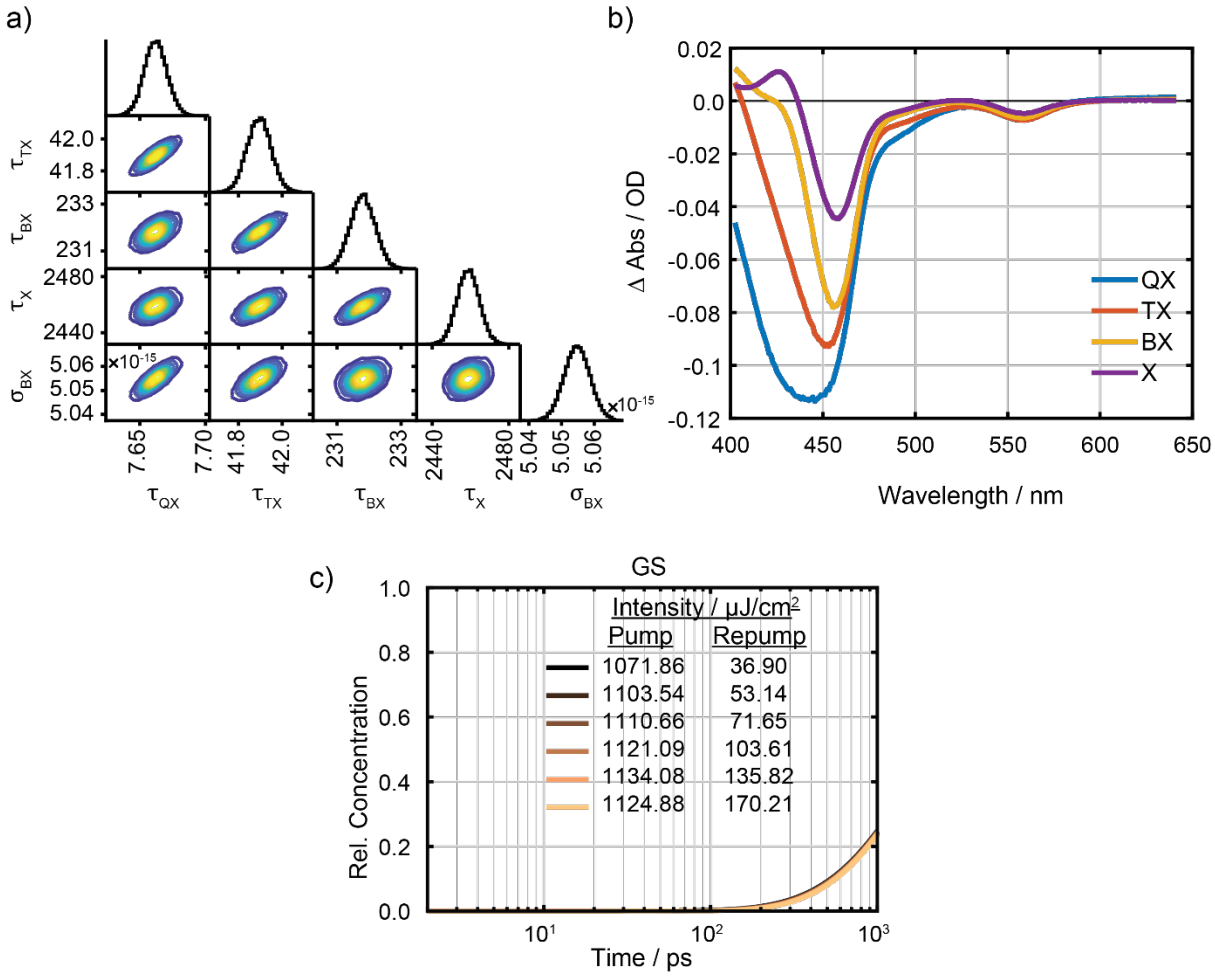

Figure S8. MCMC modelling of biexciton re-excitation (70 ps pump-repump delay) experimental data. (a) Corner plot of the posterior probability distribution of modelled parameters for pump intensity > 1070 μJ/cm^2 and re-pump intensity ranging from ~37 – 170 μJ/cm^2, (b) species associated spectra of modelled multiexciton species in ppp-TA data, and (c) Concentration profile of modelled ground state species, remaining concentration profiles are shown in main text. Each curve in b&c has been plotted from 100 random samples drawn from the MCMC sampling.

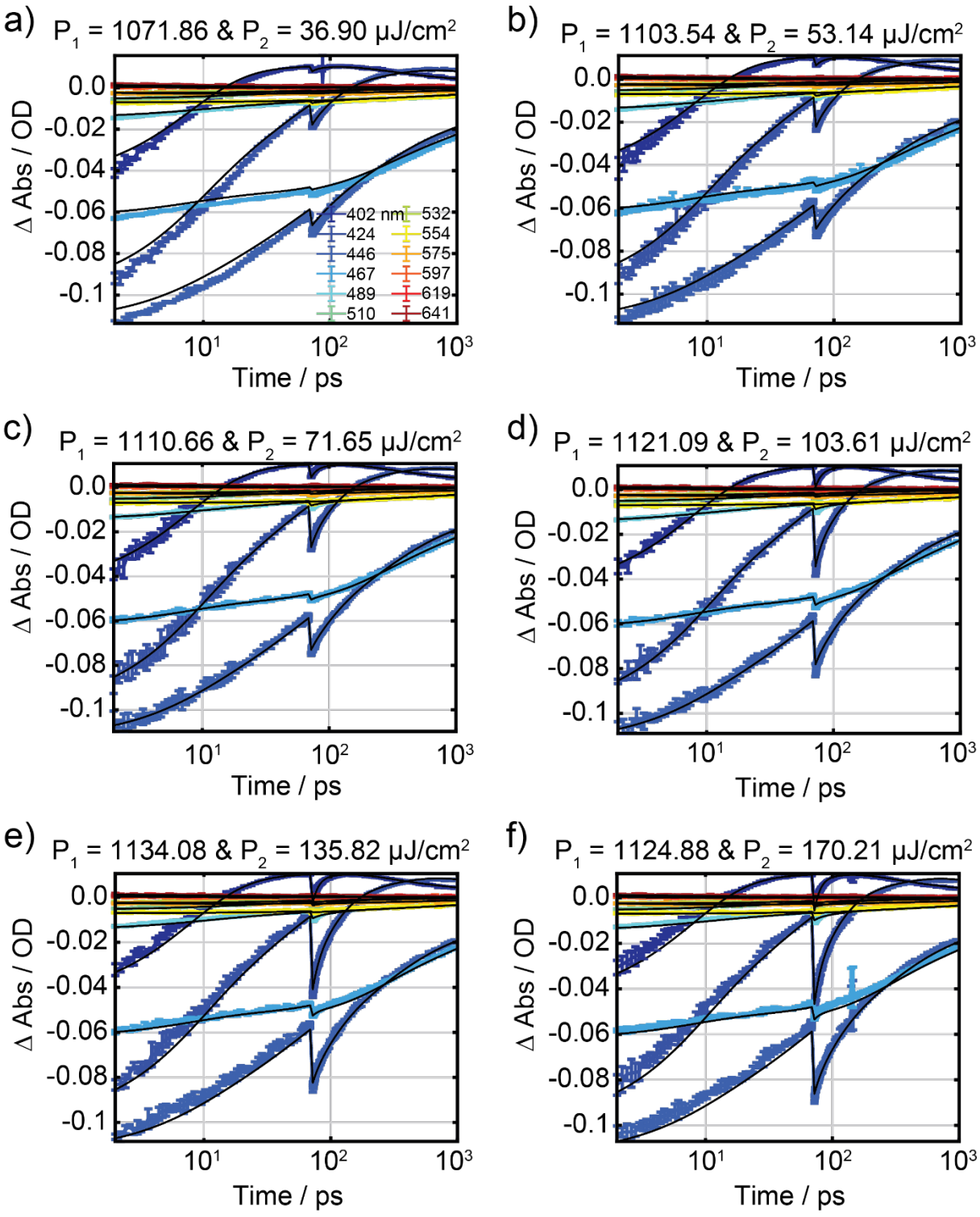

Figure S9. (a-f) Kinetics fits drawn from MCMC sampling of target model for biexciton re-excitation (70 ps pump-repump delay). Each panel shows the experimental data with their standard

deviation over at least 4 scans, and black lines represent the kinetic fit traces at that pump/repump intensity. The fit lines are plotted by drawing 100 random samples from the Markov Chain overlaid on top of each other with the same colour and linewidth to visually show the deviations among randomly drawn samples.

Experimental results – 9 ps re-excitation

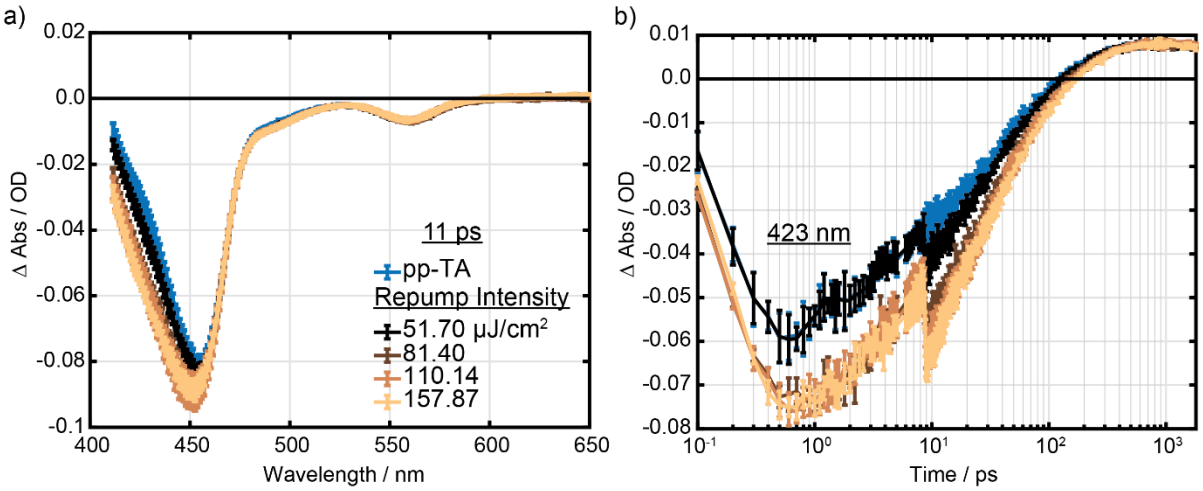

Figure S10. ppp-TA of CdSe@CdS nanorods for triexciton re-excitation. A time delay of 9 ps is fixed between the pump and the repump pulse. (a) repump intensity dependent ppp-TA spectrum at 11 ps of initial excitation (i.e. 2 ps after re-excitation). The blue curve shows the pp-TA spectrum (pump intensity 1161.26 μJ/cm^2) of CdSe@CdS nanorods after 11 ps of excitation with the first pump pulse. (b) ppp-TA kinetics at 427 nm with re-excitation by the re-pump pulse of varying intensity at 9 ps of the pump excitation.

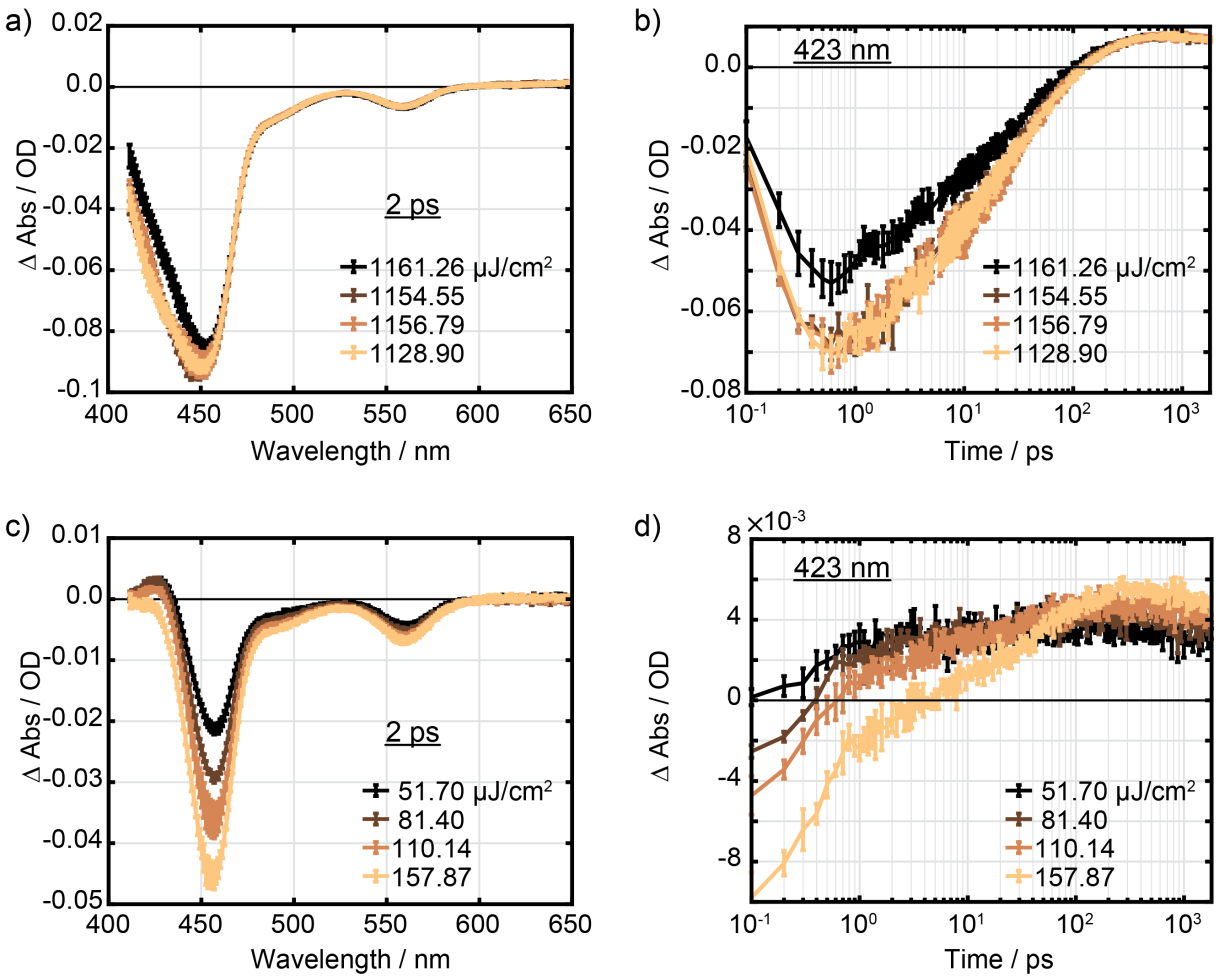

Figure S11. Reference experiments for 9 ps pump repump delay experiment shown above. pp-TA data of CdSe@CdS nanorods excited with pump (a & b) and repump pulse (c & d) only. (a,b) pp-TA spectrum of nanorods at 2 ps after the pump pulse excitation and kinetics of 423 nm band with pump intensity shown in legend. (c,d) pp-TA spectrum of nanorods at 2 ps after repump excitation and kinetics of photoinduced band at 423 nm with increasing repump intensity as shown in the legends. The time of arrival of the repump pulse is corrected by subtracting the original pump-repump delay having the excitation event at 0 ps.

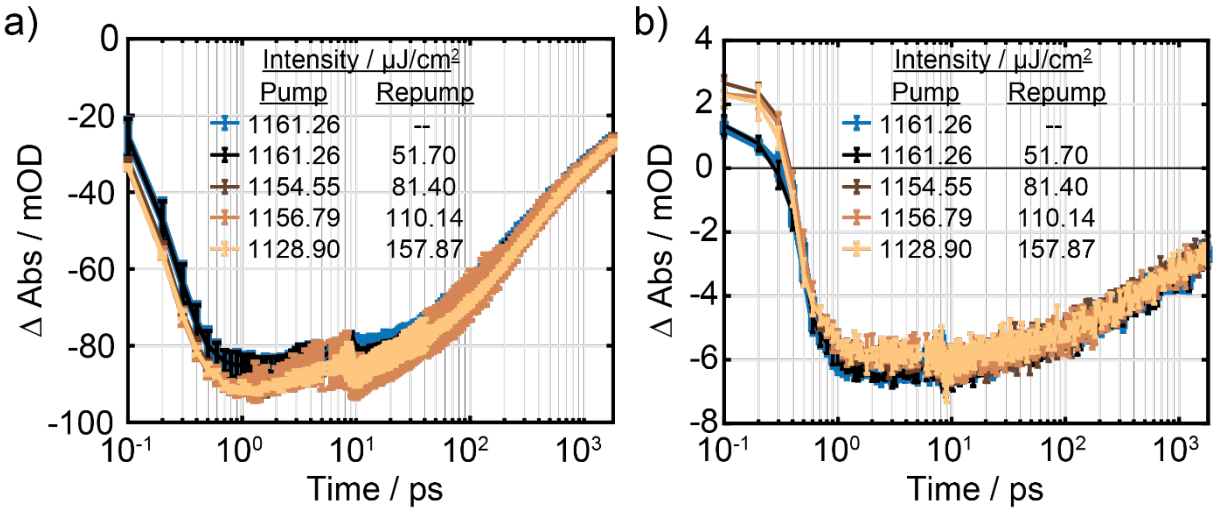

Figure S12. ppp-TA kinetics of CdS and CdSe band edge bleach features at 455 nm (a) and 553 nm (b) with varying re-excitation intensity as shown in the legend, along with a representative pp-TA kinetics of the same band shown in blue (pump intensity 1161.26 μJ/cm^2).

Fitting results – 9 ps re-excitation

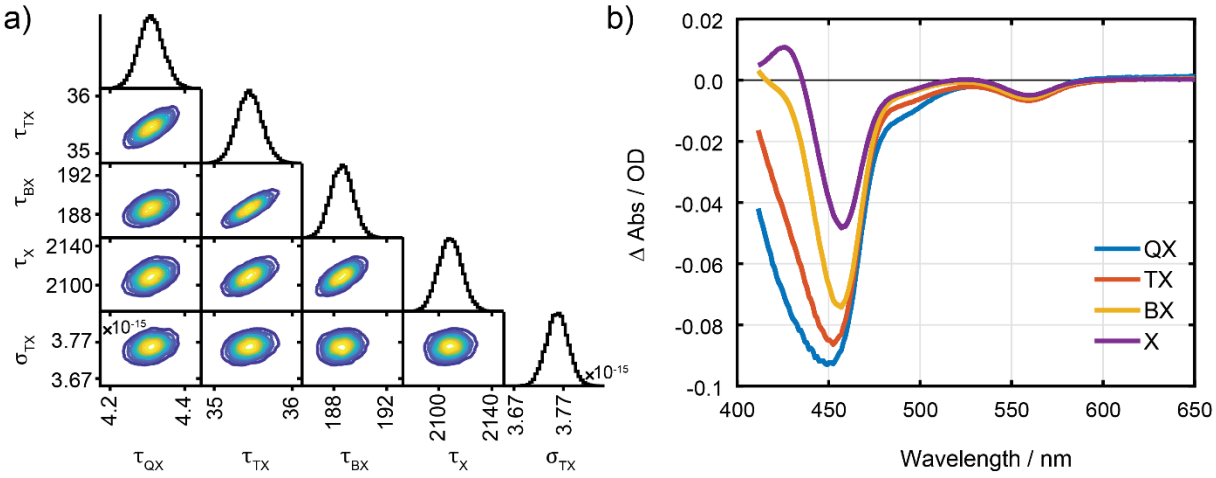

Figure S13. MCMC modelling of triexciton re-excitation (9 ps pump-repump experiment) experimental data. (a) Corner plot of the posterior probability distribution of modelled parameters for pump intensity > 1150 μJ/cm^2 and re-pump intensity ranging from ~52 – 159 μJ/cm^2, (b) species associated spectra of modelled multiexciton species in ppp-TA data. The SAS curve has been plotted from 100 random samples drawn from the MCMC sampling.

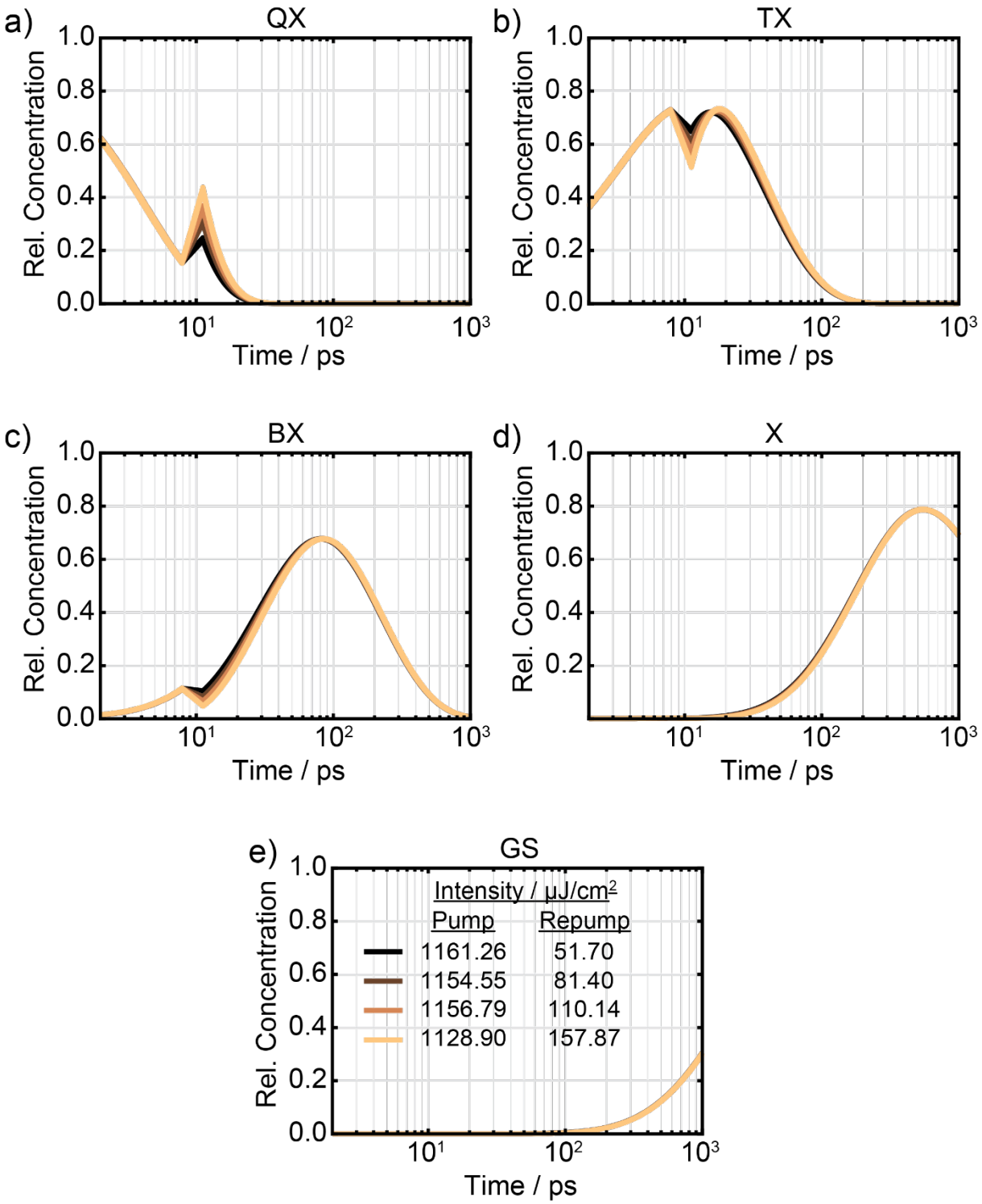

Figure S14. (a-e) The relative concentration profile of modelled tetra-, tri-, bi-, monoexciton and

ground state species, respectively, for 9 ps pump-repump experiment. Each curve has been plotted from 100 random samples drawn from the MCMC sampling.

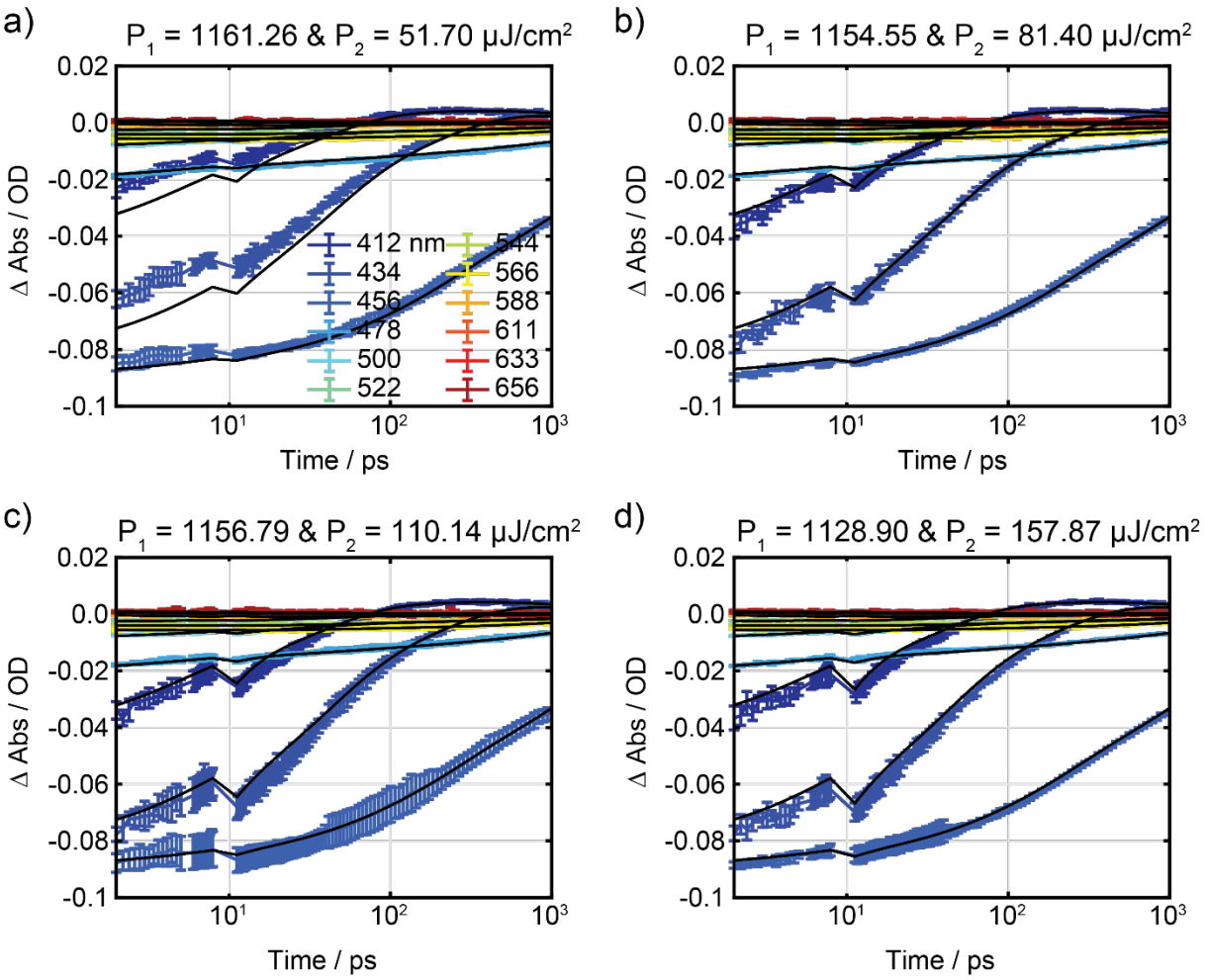

Figure S15. Kinetics fits drawn from MCMC sampling of target model for triexciton re-excitation (9 ps pump-repump experiment). Each panel shows the experimental data with their standard deviation over at least 4 scans, and black lines represent the kinetic fit traces at that pump/repump intensity. The fit lines are plotted by drawing 100 random samples from the Markov Chain overlaid on top of each other with the same colour and linewidth to visually show the deviations among randomly drawn samples.

References

(1) Wu, K.; Rodríguez-Córdoba, W. E.; Liu, Z.; Zhu, H.; Lian, T. Beyond Band Alignment: Hole Localization Driven Formation of Three Spatially Separated Long-Lived Exciton States in CdSe/CdS Nanorods. *ACS Nano* **2013**, *7* (8), 7173–7185. https://doi.org/10.1021/nn402597p.

(2) Micheel, M.; Liu, B.; Wächtler, M. Influence of Surface Ligands on Charge-Carrier Trapping and Relaxation in Water-Soluble Cdse@cds Nanorods. *Catalysts* **2020**, *10* (10), 1–23. https://doi.org/10.3390/catal10101143.

(3) Klimov, V. I.; Mikhailovsky, A. A.; McBranch, D. W.; Leatherdale, C. A.; Bawendi, M. G. Quantization of Multiparticle Auger Rates in Semiconductor Quantum Dots. *Science* **2000**, *287* (5455), 1011–1014. https://doi.org/10.1126/science.287.5455.1011.

(4) Klimov, V. I.; McGuire, J. A.; Schaller, R. D.; Rupasov, V. I. Scaling of Multiexciton Lifetimes in Semiconductor Nanocrystals. *Phys. Rev. B* **2008**, *77* (19). https://doi.org/10.1103/PhysRevB.77.195324.

(5) K. Kumar and M. Wächtler, Spectral and dynamical properties of multiexcitons in semiconductor nanorods, *Nanoscale*, DOI:10.1039/d4nr04692g.

(6) M. N. Ashner, S. W. Winslow, J. W. Swan and W. A. Tisdale, Markov Chain Monte Carlo Sampling for Target Analysis of Transient Absorption Spectra, *J. Phys. Chem. A*, 2019, **123**, 3893–3902.